Limited role for methane in the mid-Proterozoic greenhouse

Stephanie L. Olson[a,b,1], Christopher T. Reinhard[a,c], and Timothy W. Lyons[a,b]

[a]NASA Astrobiology Institute, University of California, Riverside, CA 92521; [b]Department of Earth Science, University of California, Riverside, CA 92521; and [c]School of Earth and Atmospheric Sciences, Georgia Institute of Technology, Atlanta, GA 30332

Edited by Mark H. Thiemens, University of California, San Diego, La Jolla, CA, and approved August 5, 2016 (received for review May 26, 2016)

Pervasive anoxia in the subsurface ocean during the Proterozoic may have allowed large fluxes of biogenic CH_4 to the atmosphere, enhancing the climatic significance of CH_4 early in Earth's history. Indeed, the assumption of elevated pCH_4 during the Proterozoic underlies most models for both anomalous climatic stasis during the mid-Proterozoic and extreme climate perturbation during the Neoproterozoic; however, the geologic record cannot directly constrain atmospheric CH_4 levels and attendant radiative forcing. Here, we revisit the role of CH_4 in Earth's climate system during Proterozoic time. We use an Earth system model to quantify CH_4 fluxes from the marine biosphere and to examine the capacity of biogenic CH_4 to compensate for the faint young Sun during the "boring billion" years before the emergence of metazoan life. Our calculations demonstrate that anaerobic oxidation of CH_4 coupled to SO_4^{2-} reduction is a highly effective obstacle to CH_4 accumulation in the atmosphere, possibly limiting atmospheric pCH_4 to less than 10 ppm by volume for the second half of Earth history regardless of atmospheric pO_2. If recent pO_2 constraints from Cr isotopes are correct, we predict that reduced UV shielding by O_3 should further limit pCH_4 to very low levels similar to those seen today. Thus, our model results likely limit the potential climate warming by CH_4 for the majority of Earth history—possibly reviving the faint young Sun paradox during Proterozoic time and challenging existing models for the initiation of low-latitude glaciation that depend on the oxidative collapse of a steady-state CH_4 greenhouse.

faint young Sun | boring billion | Snowball Earth | methane | oxygenation

A dearth of glacial deposits during much of the Proterozoic is traditionally interpreted as evidence that Earth's surface was as warm as, or warmer than, modern Earth throughout the mid-Proterozoic, 1.8 to 0.8 billion years ago (Ga) (1). This relatively warm climate state has conventionally been considered to require enhanced greenhouse warming to compensate for reduced solar luminosity early in Earth's history (2, 3). Although the composition of the ancient greenhouse is still debated, the temporal proximity of extensive, low-latitude glaciation and oxygenation in the Paleoproterozoic (2.5 Ga to 1.6 Ga) supports speculation that a reduced greenhouse gas, such as biogenic CH_4, played an important role in the Precambrian climate system (1, 4). This relationship has been envisaged in two ways for the Paleoproterozoic Snowball glaciations: (*i*) the Paleoproterozoic Great Oxidation Event (GOE) rapidly eroded a potent CH_4 greenhouse, and oxidative collapse of the CH_4 reservoir allowed the Earth system to plunge into snowball glaciation (5); or (*ii*) declining biogenic CH_4 fluxes allowed the collapse of a CH_4 greenhouse, extreme climate perturbation, and the initial rise of atmospheric O_2 by reducing the atmospheric sink for O_2 (6, 7). Several authors have similarly suggested that the oxidative collapse of a CH_4 greenhouse could have also triggered climate destabilization during the Neoproterozoic (1.0 Ga to 0.54 Ga) if biogenic CH_4 fluxes were elevated throughout the Proterozoic Eon, as assumed before the GOE (8–11).

Despite its conceptual convenience, the existence and/or effectiveness of a CH_4 greenhouse at any time during the Proterozoic remains speculative. Although relatively small surface oxidant reservoirs (e.g., O_2 and SO_4^{2-}) during Proterozoic time may have allowed large CH_4 fluxes from the marine biosphere (9), the geologic record does not provide quantitative constraints on either CH_4 fluxes or the CH_4 content of the atmosphere, and some models suggest only modest CH_4 accumulation in the Proterozoic atmosphere compared with the Archean (12, 13). Characterization of the Proterozoic greenhouse is further complicated by (*i*) strong nonlinearity in biospheric CH_4 fluxes as a function of marine SO_4^{2-} concentrations, which arises because CH_4 consumption and CH_4 production are increased and decreased, respectively, with increasing $[SO_4^{2-}]$ (14, 15); and (*ii*) strong nonlinearity in the atmospheric lifetime of CH_4 as a function of atmospheric pO_2, which reflects the competing effects on CH_4 stability from O_2 content of the ocean–atmosphere system and correspondingly greater UV shielding by O_3 in oxidizing atmospheres (16, 17). In other words, both the production and preservation of CH_4 are disfavored by high levels of O_2, but some low threshold level of O_2 enhances CH_4 preservation in the atmosphere because its photochemical destruction is muted when a protective O_3 layer is well established (16, 17). These challenges for quantifying atmospheric CH_4 (pCH_4) are exacerbated by the nonlinear relationships between atmospheric pO_2, crustal sulfide oxidation, and marine pyrite burial, muddling the relationship between atmospheric pO_2 and oceanic $[SO_4^{2-}]$ (18, 19). Thus, the quantitative relationships between O_2, SO_4^{2-}, and CH_4, on a global scale, are poorly understood for much of Earth's history.

Potential Constraints for Proterozoic Methane

In the modern ocean, SO_4^{2-}, not O_2, is the primary oxidant for CH_4 because of the coupling between SO_4 and CH_4 during anaerobic oxidation of methane (AOM) by microbes. Consequently,

Significance

Proterozoic climate dynamics, including both remarkable climate stability during the mid-Proterozoic and extreme low-latitude glaciation in the Neoproterozoic, must be understood in the framework of evolving oxidant reservoirs throughout the Precambrian. We present Earth system model simulations showing that recent constraints on atmospheric oxygen and oceanic sulfate during Proterozoic time have profound implications for marine methane cycling and the accumulation of methane in the atmosphere. Our model results challenge the paradigm of persistently elevated methane during the Precambrian, thus extending the relevance of the faint young Sun paradox throughout the Proterozoic. In light of the possibility of low methane during the mid-Proterozoic, we also suggest a conceptual model for the relationship between oxygenation, methane, and Neoproterozoic Snowball Earth events.

Author contributions: S.L.O. and C.T.R. designed research; S.L.O. performed research; S.L.O. and C.T.R. analyzed data; and S.L.O., C.T.R., and T.W.L. wrote the paper.

The authors declare no conflict of interest.

This article is a PNAS Direct Submission.

[1]To whom correspondence should be addressed. Email: solso002@ucr.edu.

This article contains supporting information online at www.pnas.org/lookup/suppl/doi:10.1073/pnas.1608549113/-/DCSupplemental.

freshwater, terrestrial ecosystems (e.g., wetlands) are the most important source of CH_4 to the modern atmosphere (excluding anthropogenic sources) because the vast quantity of CH_4 produced deep within reducing marine sediments does not readily evade oxidation in overlying SO_4^{2-}-rich pore waters (20). Quantitative isotopic constraints on seawater SO_4^{2-} concentrations limit Proterozoic [SO_4^{2-}] to only a few millimoles per liter (21), or possibly several hundred micromoles per liter (22)—a small fraction of the 28 mM characteristic of the modern ocean. Although less than ~10% of the modern marine SO_4^{2-} inventory is certainly low in relative terms, a seawater SO_4^{2-} concentration of 1 mM still carries a far greater electron accepting capacity than the entire O_2 reservoir of the generally well-oxygenated modern ocean. Thus, even at comparatively low concentrations, SO_4^{2-} in pore waters and in an anoxic Proterozoic water column could have been a major obstacle preventing biogenic CH_4 from escaping the ocean environment and entering the atmosphere.

Early arguments for elevated pCH_4 during the Proterozoic were predicated on the notion that surface CH_4 fluxes could have been >10× to 20× modern values due to enhanced methanogenesis and complete inhibition of methanotrophy under low [SO_4^{2-}] conditions (9, 10), but this assumption has been challenged both experimentally and through the recognition of extensive anaerobic CH_4 recycling in modern analog environments. For example, efficient microbial oxidation of CH_4 coupled to SO_4^{2-} reduction has been documented at SO_4^{2-} concentrations as low as 100 μM (23), which is potentially much lower than the [SO_4^{2-}] conditions that typified the Proterozoic ocean (21). Recent work has also shown that CH_4 oxidation can be metabolically coupled to a range of alternate electron acceptors [e.g., Mn(III/IV) and Fe(III)] in freshwater lake systems (24) and in SO_4^{2-}-deficient marine sediments (25). These metabolic pathways are theoretically more energetically favorable than SO_4^{2-}-based AOM and are likely to have been important for Precambrian CH_4 cycling given the apparent abundance of Fe and Mn in the Precambrian ocean (23, 26); however, there have been few attempts to include these metabolic sinks for CH_4 in quantitative biogeochemical models, with attempts, to date, focusing on photochemical models that do not explicitly resolve redox cycling within the ocean (23, 27).

Somewhat counterintuitively, low pO_2 in the Proterozoic may have also been an obstacle to CH_4 accumulation in the atmosphere due to strongly diminished UV shielding by O_3 at low pO_2—which would act to greatly decrease the photochemical lifetime of atmospheric CH_4. For this reason, atmospheres with low pO_2 can be more oxidizing toward CH_4 than higher pO_2 atmospheres (16, 17). Thus, there is an optimization of the lifetime of atmospheric CH_4 associated with having sufficient O_2 to promote UV shielding by O_3 but at O_2 levels still low enough to minimize oxidative CH_4 destruction. Previous models that have suggested the existence of a CH_4 greenhouse during the Proterozoic have assumed that pO_2 stabilized at, or above, ~10% present atmospheric levels (PAL) following the GOE (9), but several diverse proxy records collectively indicate that pO_2 may have eventually stabilized at much lower levels than those seen during the GOE and associated Lomagundi event (28). Recently, the absence of Cr isotope fractionation in mid-Proterozoic marine sediments suggests that atmospheric pO_2 may have been as low as 0.1% PAL, an order of magnitude lower than envisioned by some authors (29). Consequently, it is possible that previous attempts to characterize the Proterozoic greenhouse have overestimated the lifetime for atmospheric CH_4.

Ocean-Resolving Methane Cycle Model

In response to recent revelations regarding the high efficiency of anaerobic CH_4 oxidation under low [SO_4^{2-}] conditions (23–25) and refined constraints on atmospheric O_2 levels during the mid-Proterozoic (29), we have revisited the role of CH_4 in mid-Proterozoic climate stabilization and Neoproterozoic climate perturbation. Our calculations were performed using the grid-enabled integrated Earth system model (GENIE), an Earth system model of intermediate complexity. GENIE considers a 3D marine biosphere, including nutrient-limited export production, aerobic respiration, sulfate reduction, and methanogenesis. The marine biogeochemical module also includes aerobic methanotrophy and sulfide oxidation (see ref. 30 for a detailed description). The ocean is divided as a 36 × 36 equal-area grid with 16 depth layers, and the ocean system is coupled to a 2D energy and moisture balance model, a sea ice model, and a 2D model for

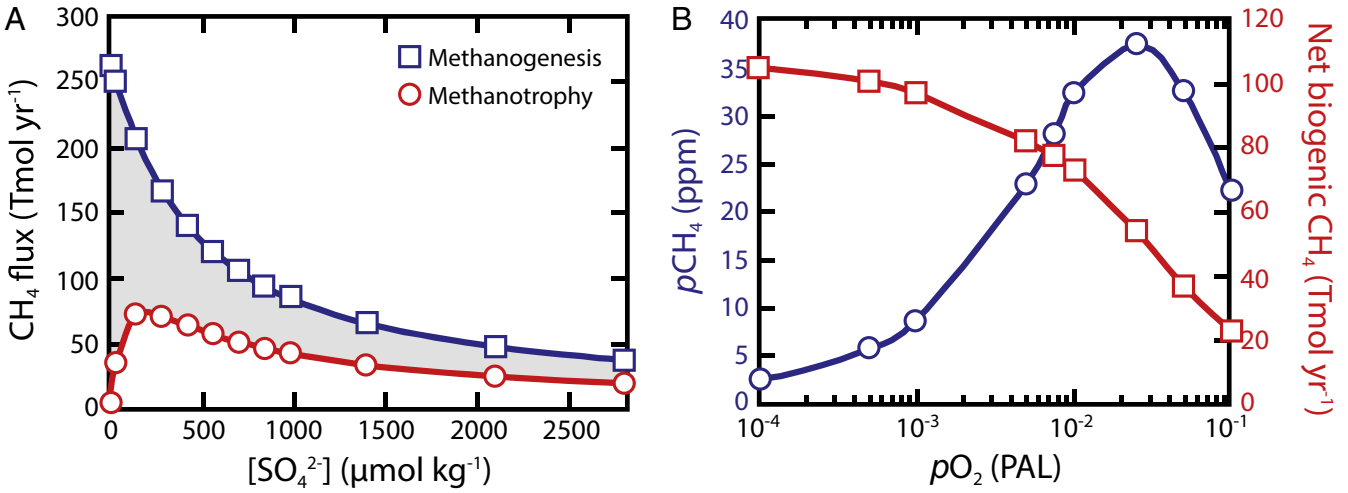

Fig. 1. Oxidant controls on CH_4 cycling. (*A*) CH_4 production flux (methanogenesis; blue squares) and CH_4 consumption flux (the sum of aerobic methanotrophy and AOM; red circles) as a function of marine SO_4^{2-}. The difference between methanogenesis and methanotrophy is equal to the net biogenic CH_4 flux (i.e., the flux of CH_4 that enters the atmosphere through sea–air exchange). Note that the SO_4^{2-} experiments shown here assume $pO_2 = 10^{-3}$ PAL (29). (*B*) Net biogenic CH_4 flux to the atmosphere (red squares) and atmospheric pCH_4 (blue circles) as a function of atmospheric pO_2. Net biogenic CH_4 production declines with increasing O_2 due to enhanced methanotrophic oxidation of CH_4, but CH_4 accumulation in the atmosphere increases despite reduced CH_4 supply due to the establishment of an increasingly effective O_3 layer (see figure 7 from ref. 34). Note that pO_2 experiments shown here assume [SO_4^{2-}] = 280 μM.

the calculation of atmospheric chemistry and spatially resolved, bidirectional sea–air exchange fluxes (31).

For our Proterozoic simulations, we have expanded GENIE's representation of the CH_4 cycle compared with previously published versions of the model. In particular, we have (*i*) parameterized dynamic calculation of CH_4 photooxidation (incorporated after ref. 17); (*ii*) refined the competition between methanogens and sulfate reducers (improved from ref. 32); and (*iii*) added AOM coupled to SO_4^{2-} reduction, the rate law for which we derived from radio-labeled CH_4 oxidation rates and chemical profiles from the anoxic water column of the Black Sea (Eq. **S1**) (33). In combination, these upgrades add strong nonlinearity to both CH_4 fluxes and CH_4 accumulation as a function of oxidant availability, allowing for an oceanographically realistic calculation of CH_4 cycling during oxidant-deficient intervals of Earth history.

We calculated steady-state biogenic CH_4 fluxes and resulting atmospheric pCH_4 for >75 model configurations, differing primarily in the prescribed sizes of their surface oxidant reservoirs (e.g., O_2 and SO_4^{2-}). We systematically quantified the influence of pO_2 (from 10^{-5} PAL to 10^{-1} PAL) and oceanic [SO_4^{2-}] (from 0 to 2.8 mM). We then performed a wide range of sensitivity analyses (*Supporting Information*), starting from our baseline oxidant levels (10^{-3} PAL pO_2, 280 μM SO_4^{2-}) and examining the effects of varying (*i*) prescribed CH_4 fluxes from terrestrial environments (0 Tmol $CH_4{\cdot}y^{-1}$ to 22 Tmol $CH_4{\cdot}y^{-1}$), (*ii*) the oceanic PO_4^{3-} inventory (i.e., export production, from 0.25× to 2× modern), (*iii*) whether or not N limitation is considered, (*iv*) the depth distribution of organic carbon (C_{org}) remineralization, (*v*) the rate constants for both aerobic and anaerobic microbial CH_4 oxidation, and (*vi*) the half-saturation constant for SO_4^{2-} reduction. We also explored model sensitivity to the parameterization of CH_4 oxidation within the atmosphere.

Importantly, our modeling experiments were designed to conservatively err in favor of overestimating pCH_4 by calculating generous CH_4 production fluxes while minimizing CH_4 destruction. In our baseline model, we assume complete remineralization of exclusively P-limited export production in a closed ocean–atmosphere system; because this base model stipulates a modern PO_4^{3-} inventory while neglecting potential N stress and C removal through organic burial, these calculations tend to overestimate the amount of organic matter remineralized via methanogenesis. This potential for overestimating CH_4 production is further amplified by our use of a relatively high half-saturation constant for SO_4^{2-} reduction (500 μM SO_4^{2-}), which effectively reduces the competitive advantage of SO_4^{2-} reducers over methanogens. Furthermore, because we neglect anaerobic oxidation of CH_4 coupled to electron acceptors other than SO_4^{2-} (e.g., oxidized Fe and Mn), it is unlikely that we overestimate CH_4 oxidation by the marine biosphere. Consequently, the sea-to-air CH_4 fluxes and subsequent pCH_4 calculations presented here should be considered conservative upper limits (see *Supporting Information* for further details).

Oxidant Controls on Methane Cycling

We find that, during the Proterozoic, SO_4^{2-} would have been the primary control on biogenic CH_4 fluxes from the ocean, not unlike today. Methane production by methanogenesis rapidly declines as SO_4^{2-} reduction, the more energetically favorable metabolism, becomes increasingly competitive at higher [SO_4^{2-}] and remineralizes a correspondingly greater fraction of organic material exported from the surface ocean. Meanwhile, CH_4 destruction via AOM increases with increasing [SO_4^{2-}], until low CH_4 availability ultimately limits AOM kinetics and slows CH_4 oxidation. The combined result of these effects is that net biogenic CH_4 fluxes to the atmosphere plummet as oceanic [SO_4^{2-}] increases (Fig. 1*A*), and the extreme sea-to-air CH_4 fluxes suggested by Pavlov et al. (9) are not achievable for any of our model configurations. Thus, relatively modest oceanic SO_4^{2-} levels can, in principle, preclude significant warming by CH_4 on early Earth, regardless of atmospheric pO_2.

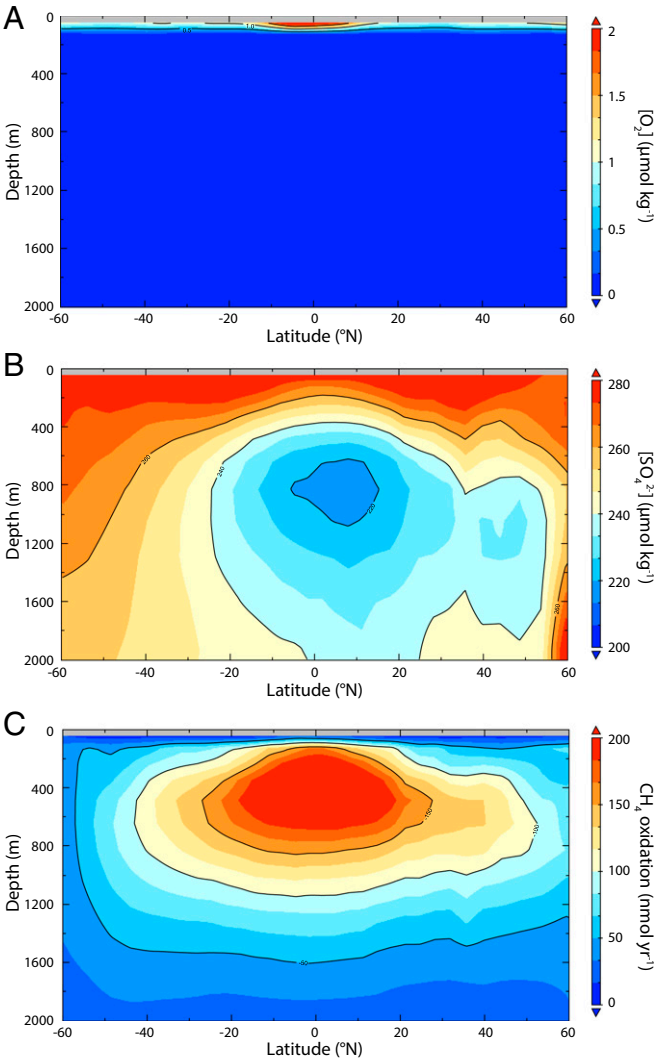

Fig. 2. (*A*) Zonally and annually averaged dissolved O_2 profile. The distribution of dissolved O_2 for our standard Proterozoic ocean is strikingly similar to the O_2 landscape of the Archean ocean (32). Although the photic zone is widely supersaturated with respect to O_2, the subsurface ocean is pervasively anoxic under Proterozoic conditions, and aerobic methanotrophy is restricted to the surface ocean. (*B*) Zonally and annually averaged SO_4^{2-} profile. SO_4^{2-} is strongly heterogeneous in the subsurface ocean. Where organic fluxes are elevated and water masses are older, pronounced SO_4^{2-} minimum zones are established. These environments are directly analogous to modern O_2 minimum zones (Fig. S1). Note that, where [SO_4^{2-}] is plotted elsewhere, globally uniform concentrations are not implied; instead, [SO_4^{2-}], as in Fig. 1 and Fig. 3, represents the global average concentration of SO_4^{2-}. (*C*) Zonally and annually averaged CH_4 oxidation rates. Contours represent the combined rates of aerobic and anaerobic methanotrophy. Generally, CH_4 oxidation rates mirror CH_4 concentrations (Fig. S1). For reference, the modern rate of CH_4 oxidation in the anoxic water column of the Black Sea is ~600 nmol $kg^{-1}{\cdot}y^{-1}$ (33). Like the Black Sea, CH_4 oxidation is dominated by anaerobic metabolism.

At higher atmospheric O_2 levels, net biogenic CH_4 fluxes also decline as a consequence of higher rates of methanotrophy—both aerobic (i.e., through direct metabolic consumption of CH_4 with O_2) and anaerobic (i.e., through more effective regeneration of SO_4^{2-} via S^{2-} reoxidation). Globally, however, aerobic methanotrophy is quantitatively much less significant than AOM because, when pO_2 is low, oxygenation and aerobic methanotrophy are spatially restricted to the photic zone (Fig. 2*A*), which represents less than a few percent of the ocean by volume, whereas

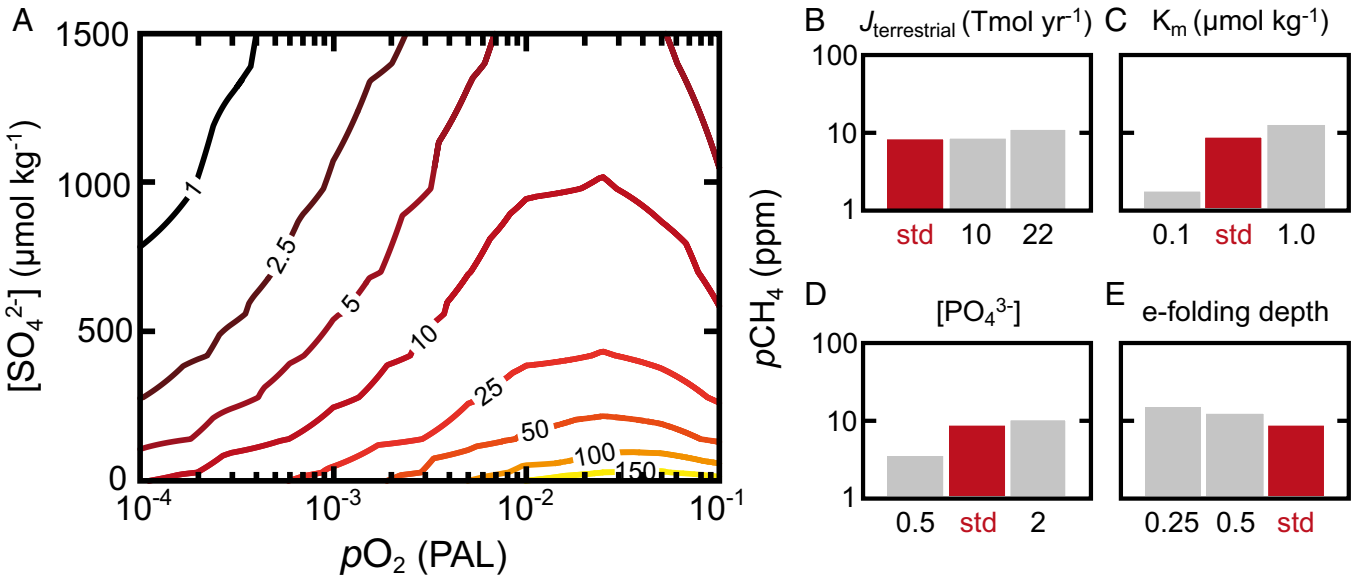

Fig. 3. (*A*) The pCH_4 contours for possible Proterozoic oxidant conditions. For reference, 100 ppmv CH_4 to 300 ppmv CH_4 is required to reconcile the absence of glaciation with the faint young Sun (9), but this value is almost certainly an underestimate (37), unless warming by pCO_2 was higher than that calculated by the current generation of 1D atmospheric models. A CH_4 greenhouse is favored by $pO_2 \approx 1$ to 10% PAL, whereas $pCH_4 > 10$ ppmv is precluded for $[SO_4^{2-}] > 1$ mM. (*B*–*E*) The pCH_4 sensitivity to select parameters. The red bar in each panel represents our standard model configuration, and the gray bars represent pCH_4 results for simulations that were run under identical oxidant conditions and differ with respect to (*B*) the flux of CH_4 from terrestrial environments, (*C*) the half-saturation constant for SO_4^{2-} reduction, (*D*) the oceanic PO_4^{3-} inventory, and (*E*) the depth distribution of organic matter remineralization. Model sensitivity to each of these parameters is small compared with the influence of surface oxidant conditions (*A*). Unless otherwise specified, the values on the *x* axis of each panel are presented as times standard value (red bar). See Table S1 for full sensitivity results.

AOM occurs throughout the ocean interior in closer association with CH_4 production (Fig. 2*C*). Consequently, CH_4 oxidation linked to SO_4^{2-} reduction in a broadly anoxic Proterozoic ocean greatly exceeds CH_4 oxidation by O_2 globally. The influence of atmospheric pO_2 on aqueous CH_4 oxidation is further muted when atmospheric pO_2 is low because the surface ocean—the site of O_2 production—is widely supersaturated with O_2 with respect to the atmosphere when pO_2 is less than ~2.5% PAL. Under these conditions, sea–air exchange of O_2 is effectively unidirectional, which partially decouples atmospheric pO_2 from dissolved O_2 and aerobic metabolism in the surface ocean.

Despite limited influence on net biogenic CH_4 fluxes, atmospheric pO_2 exerts strong control on the accumulation of CH_4 in the atmosphere when $[SO_4^{2-}]$ is sufficiently low to allow significant CH_4 escape to the atmosphere. For the range of atmospheric pO_2 that is consistent with the absence of mass-independent fractionation of S isotopes and unfractionated Cr in Proterozoic marine sediments (10^{-5} to 10^{-3} PAL) (29, 34), the atmospheric lifetime of CH_4 increases with increasing pO_2 as the result of an increasingly effective O_3 UV shield (Fig. S2). This effect ultimately dominates at steady state over enhanced methanotrophic oxidation of CH_4 when pO_2 is very low, with the result that atmospheric pCH_4 is greater despite reduced production of CH_4 in an increasingly oxygenated Earth system. For example, as pO_2 increases from 0.1 to 1% PAL, net biogenic CH_4 production declines more than 20% whereas atmospheric pCH_4 increases more than 200% as a consequence of muted photochemistry and a correspondingly greater lifetime for atmospheric CH_4 (Fig. 1*B*).

Combining the opposing effects of $[SO_4^{2-}]$ and pO_2, we find that a robust steady-state CH_4 greenhouse is plausible for only a very narrow window of pO_2–$[SO_4^{2-}]$ parameter space (Fig. 3*A*). Atmospheric pCH_4 values greater than ~10 ppm by volume (ppmv) do not occur for $[SO_4^{2-}] > 1$ mM, whereas pCH_4 values greater than ~100 ppmv are restricted to pO_2 between 1 and 10% PAL. Thus, substantial accumulation of CH_4 in the atmosphere requires the unique combination of exceptionally low $[SO_4^{2-}]$(<<1 mM), which allows sufficiently large CH_4 fluxes from the marine biosphere, and relatively high pO_2 (1 to 10% PAL), which optimizes the atmospheric lifetime of CH_4. Although uncertainties remain regarding the coevolution of pO_2 and marine $[SO_4^{2-}]$, this requirement for modest pO_2 and very low SO_4^{2-} is not consistent with the most recent $[SO_4^{2-}]$ and pO_2 proxy records and likely would have been difficult to maintain over geologic timescales considering the coupling between atmospheric pO_2, crustal sulfide oxidation, and SO_4^{2-} fluxes. These conclusions regarding oxidant controls on pCH_4 are insensitive to uncertainty in other model parameters (Fig. 3 *B*–*E* and Table S1), indicating that our salient results are robust, and these constraints challenge the paradigm of persistently elevated pCH_4 throughout the Precambrian.

Consequences for Proterozoic Climate

Elevated pCH_4 on the order of 100 ppmv could provide ~6 K of greenhouse warming, which would substantially, although not completely, compensate for reduced solar luminosity if Proterozoic Earth was persistently warmer than today (10); thus we consider ~6 K to be the minimum radiative deficit implied by our model if the Proterozoic $[SO_4^{2-}]$ approached 1 mM or if pO_2 was lower than previously appreciated. This deficit is a substantial one that is difficult to reconcile with the absence of glaciation and the suggestion that Proterozoic pCO_2 was <10× modern (35).

Other reduced greenhouse gases that are not explicitly considered by our model may have bolstered the mid-Proterozoic greenhouse, helping to alleviate the radiative deficit produced by low atmospheric pCH_4. Most notably, atmospheric levels of nitrous oxide (N_2O) during the Proterozoic may have been much higher if widespread euxinia limited Cu availability and inhibited effective conversion of N_2O to N_2 during the final stage of denitrification (36), potentially yielding ~5 K of supplemental warming (10). Although SO_4^{2-} would not severely throttle N_2O fluxes, N_2O—like CH_4—is rapidly photolyzed at low pO_2. Nitrous oxide, therefore, is only a viable greenhouse contributor for a partial range of the proposed pO_2 conditions for the

Proterozoic (10). Higher hydrocarbons, particularly ethane (C_2H_6), can be photochemically produced from CH_4 and may have been important for regulating the climate of Archean Earth (37), but our model results generally preclude the elevated pCH_4:pCO_2 conditions required for substantial hydrocarbon polymerization. Thus, greenhouse contributions from other hydrocarbons are unlikely during Proterozoic time.

In combination with evidence for relatively low pCO_2 during much of the Proterozoic (35), we conclude that the faint young Sun paradox may still be a problem for the Proterozoic if relatively high CH_4 levels are precluded by current estimates of oceanic SO_4^{2-} and/or atmospheric pO_2. Continued exploration of the metabolic limitations of CH_4 oxidizing consortia (11), revised pCO_2 calculations, or more realistic consideration of heat transport in increasingly sophisticated 3D coupled climate models may eventually reconcile our suggestion of low pCH_4 with clement conditions during the mid-Proterozoic, but, given current constraints on the warming potential of CO_2 during Proterozoic time, the paradox remains unresolved.

Given the possibility that baseline Proterozoic pCH_4 was much lower than previously envisioned, the role of CH_4 in triggering Neoproterozoic climate collapse also requires revisiting. Several authors have previously suggested that the oxidative collapse of a CH_4 greenhouse was involved in the initiation of Neoproterozoic snowball glaciations (1, 8, 9). Indeed, emerging trace metal proxies suggest atmospheric oxygenation in advance of the glaciation (29, 38), despite unclear evidence for oxygenation within the marine realm (39–41). The climatic consequences of the oxygenation of a low pCH_4 atmosphere, however, have not been previously considered.

We suggest that a Neoproterozoic oxygenation event might have triggered a CH_4-based climate collapse, despite low steady-state pCH_4, as a result of the vastly differing timescales over which photochemical, biological, and weathering processes modulate Earth's greenhouse. For example, the immediate consequence of an atmospheric oxygenation event would be an increase in the photochemical lifetime of CH_4 via UV shielding by O_3, and thus an initial increase in atmospheric pCH_4. Subsequent destabilization of CH_4 hydrates as the result of a warming climate may amplify this initial accumulation of CH_4 in the atmosphere (12, 42). The resulting greenhouse, however, would be inherently unstable because CH_4-induced warming would promote the drawdown of CO_2 on weathering timescales (12, 42); thus, the climate system would then be vulnerable to any disruption of the CH_4 source to the atmosphere (42), including the gradual accumulation of oceanic SO_4^{2-} that would accompany oxygenation (9). A CH_4 greenhouse would also be sensitive to CH_4 instability arising as the result of either further oxygenation or even deoxygenation.

Although conceptually similar to the "methane shotgun" scenario advanced by Schrag et al. (42), our snowball initiation scenario has the advantage of eliminating the need for a large, sustained external source of CH_4 to the ocean–atmosphere system and does not rely on either enhanced biological CH_4 production or high steady-state pCH_4 before climate destabilization. Glacial initiation through the buildup and collapse of a CH_4 greenhouse in response to an oxygenation event may also provide an explanation for the enigmatic C isotope excursions of the late Neoproterozoic (12, 42). Future geochemical and model analyses that clarify the relationship between oxygenation, glaciation, and isotopic perturbation in the Neoproterozoic will be required to validate our proposed snowball scenario and could provide implicit support for our conclusion that baseline pCH_4 was very low during much of the Proterozoic.

Summary

We have shown that long-term stabilization of Earth's climate system by CH_4 is challenging for much of Earth history, despite the likelihood of greatly enhanced CH_4 cycling within the broadly anoxic Proterozoic ocean. Even at very low SO_4^{2-} concentrations, anaerobic oxidation of CH_4 in the ocean is sufficient to severely throttle CH_4 fluxes to the atmosphere, precluding the stability of an atmosphere with >100 ppmv CH_4 as previously suggested for Proterozoic Earth. If recent pO_2 constraints from Cr isotopes are correct, reduced UV shielding by O_3 may exacerbate this issue, further limiting the potential accumulation of CH_4 in the atmosphere—with the implication that mid-Proterozoic pCH_4 may not have been markedly different from the low levels present today. In this scenario, our results suggest that elevated CH_4 should not be invoked to reconcile existing constraints on the composition of the mid-Proterozoic greenhouse with the absence of glaciation in the mid-Proterozoic. Thus, the faint young Sun paradox remains unresolved.

Although our model results imply relatively low steady-state pCH_4 (<10 PAL) during the second half of Earth history, they do not preclude a significant role for O_2 and CH_4 in destabilizing the Neoproterozoic climate system. Rather than occurring as the result of the demise of a steady-state CH_4 greenhouse, we suggest that the extreme low-latitude glaciations during the Neoproterozoic are the consequence of non–steady-state CH_4–oxidant dynamics produced by the interplay of the marine biosphere, photochemistry, weathering, and climate.

ACKNOWLEDGMENTS. We thank David Catling, Tim Lenton, and an anonymous reviewer for constructive and insightful reviews. This work was supported by the National Aeronautics and Space Administration Astrobiology Institute (C.T.R. and T.W.L.), the National Science Foundation Earth-Life Transitions program (C.T.R. and T.W.L.), and the National Science Foundation Frontiers in Earth System Dynamics program (T.W.L.).

1. Kasting JF (2005) Methane and climate during the Precambrian era. *Precambrian Res* 137(3):119–129.
2. Sagan C, Mullen G (1972) Earth and Mars: Evolution of atmospheres and surface temperatures. *Science* 177(4043):52–56.
3. Walker JCG, Hays PB, Kasting JF (1981) A negative feedback mechanism for the long-term stabilization of Earth's surface temperature. *J Geophys Res* 86(C10):9776–9782.
4. Pavlov AA, Kasting JF, Brown LL, Rages KA, Freedman R (2000) Greenhouse warming by CH_4 in the atmosphere of early Earth. *J Geophys Res* 105(E5):11981–11990.
5. Kopp RE, Kirschvink JL, Hilburn IA, Nash CZ (2005) The Paleoproterozoic snowball Earth: A climate disaster triggered by the evolution of oxygenic photosynthesis. *Proc Natl Acad Sci USA* 102(32):11131–11136.
6. Zahnle KJ, Claire M, Catling D (2006) The loss of mass-independent fractionation in sulfur due to a Palaeoproterozoic collapse of atmospheric methane. *Geobiology* 4(4):271–283.
7. Konhauser KO, et al. (2009) Oceanic nickel depletion and a methanogen famine before the Great Oxidation Event. *Nature* 458(7239):750–753.
8. Catling DC, Zahnle KJ, McKay CP (2002) What caused the second rise of O_2 in the Late Proterozoic? Methane, sulfate, and irreversible oxidation. *Astrobiology* 2(4):569.
9. Pavlov AA, Hurtgen MT, Kasting JF, Arthur MA (2003) Methane-rich Proterozoic atmosphere? *Geology* 31(1):87–90.
10. Roberson AL, Roadt J, Halevy I, Kasting JF (2011) Greenhouse warming by nitrous oxide and methane in the Proterozoic Eon. *Geobiology* 9(4):313–320.
11. Shen B, et al. (2016) Molar tooth carbonates and benthic methane fluxes in Proterozoic oceans. *Nat Commun* 7:10317.
12. Bjerrum CJ, Canfield DE (2011) Towards a quantitative understanding of the late Neoproterozoic carbon cycle. *Proc Natl Acad Sci USA* 108(14):5542–5547.
13. Daines SJ, Lenton TM (2016) The effect of widespread early aerobic marine ecosystems on methane cycling and the Great Oxidation. *Earth Planet Sci Lett* 434:42–51.
14. Lovley DR, Klug MJ (1983) Sulfate reducers can outcompete methanogens at freshwater sulfate concentrations. *Appl Environ Microbiol* 45(1):187–192.
15. Boetius A, et al. (2000) A marine microbial consortium apparently mediating anaerobic oxidation of methane. *Nature* 407(6804):623–626.
16. Claire MW, Catling DC, Zahnle KJ (2006) Biogeochemical modelling of the rise in atmospheric oxygen. *Geobiology* 4(4):239–269.
17. Goldblatt C, Lenton TM, Watson AJ (2006) Bistability of atmospheric oxygen and the Great Oxidation. *Nature* 443(7112):683–686.
18. Berner RA (1989) Biogeochemical cycles of carbon and sulfur and their effect on atmospheric oxygen over Phanerozoic time. *Palaeogeogr Palaeoclimatol Palaeoecol* 75(1-2):97–122.
19. Berner RA, Petsch ST (1998) The sulfur cycle and atmospheric oxygen. *Science* 282: 1426–1427.
20. Reeburgh WS (2007) Oceanic methane biogeochemistry. *Chem Rev* 107(2):486–513.
21. Kah LC, Lyons TW, Frank TD (2004) Low marine sulphate and protracted oxygenation of the Proterozoic biosphere. *Nature* 431(7010):834–838.

22. Scott C, et al. (2014) Pyrite multiple-sulfur isotope evidence for rapid expansion and contraction of the early Paleoproterozoic seawater sulfate reservoir. *Earth Planet Sci Lett* 389:95–104.
23. Beal EJ, Claire MW, House CH (2011) High rates of anaerobic methanotrophy at low sulfate concentrations with implications for past and present methane levels. *Geobiology* 9(2):131–139.
24. Crowe SA, et al. (2011) The methane cycle in ferruginous Lake Matano. *Geobiology* 9(1):61–78.
25. Riedinger N, et al. (2014) An inorganic geochemical argument for coupled anaerobic oxidation of methane and iron reduction in marine sediments. *Geobiology* 12(2): 172–181.
26. Beal EJ, House CH, Orphan VJ (2009) Manganese- and iron-dependent marine methane oxidation. *Science* 325(5937):184–187.
27. Catling DC, Claire MW, Zahnle KJ (2007) Anaerobic methanotrophy and the rise of atmospheric oxygen. *Philos Trans A Math Phys Eng Sci* 365(1856):1867–1888.
28. Lyons TW, Reinhard CT, Planavsky NJ (2014) The rise of oxygen in Earth's early ocean and atmosphere. *Nature* 506(7488):307–315.
29. Planavsky NJ, et al. (2014) Low mid-Proterozoic atmospheric oxygen levels and the delayed rise of animals. *Science* 346(6209):635–638.
30. Ridgwell A, et al. (2007) Marine geochemical data assimilation in an efficient Earth System Model of global biogeochemical cycling. *Biogeosciences* 4(1):87–104.
31. Edwards NR, Marsh R (2005) Uncertainties due to transport-parameter sensitivity in an efficient 3-D ocean-climate model. *Clim Dyn* 24(4):415–433.
32. Olson SL, Kump LR, Kasting JF (2013) Quantifying the areal extent and dissolved oxygen concentrations of Archean oxygen oases. *Chem Geol* 362:35–43.
33. Reeburgh WS, et al. (1991) Black Sea methane geochemistry. *Deep Sea Res A* 38(Suppl 2A): S1189–S1210.
34. Pavlov AA, Kasting JF (2002) Mass-independent fractionation of sulfur isotopes in Archean sediments: Strong evidence for an anoxic Archean atmosphere. *Astrobiology* 2(1):27–41.
35. Sheldon ND (2013) Causes and consequences of low atmospheric pCO_2 in the Late Mesoproterozoic. *Chem Geol* 362:224–231.
36. Buick R (2007) Did the Proterozoic 'Canfield Ocean' cause a laughing gas greenhouse? *Geobiology* 5(2):97–100.
37. Haqq-Misra JD, Domagal-Goldman SD, Kasting PJ, Kasting JF (2008) A revised, hazy methane greenhouse for the Archean Earth. *Astrobiology* 8(6):1127–1137.
38. Pogge von Strandmann PA, et al. (2015) Selenium isotope evidence for progressive oxidation of the Neoproterozoic biosphere. *Nat Commun* 6:10157.
39. Johnston DT, et al. (2013) Searching for an oxygenation event in the fossiliferous Ediacaran of northwestern Canada. *Chem Geol* 362:273–286.
40. Kendall B, et al. (2015) Uranium and molybdenum isotope evidence for an episode of widespread ocean oxygenation during the late Ediacaran Period. *Geochim Cosmochim Acta* 156:173–193.
41. Sperling EA, et al. (2015) Statistical analysis of iron geochemical data suggests limited late Proterozoic oxygenation. *Nature* 523(7561):451–454.
42. Schrag DP, Berner RA, Hoffman PF, Halverson GP (2002) On the initiation of a snowball Earth. *Geochem Geophys Geosyst* 3(6):1–24.
43. Meyer KM, Kump LR, Ridgwell A (2008) Biogeochemical controls on photic-zone euxinia during the end-Permian mass extinction. *Geology* 36(9):747–750.
44. Pallud C, Van Cappellen P (2006) Kinetics of microbial sulfate reduction in estuarine sediments. *Geochim Cosmochim Acta* 70(5):1148–1162.
45. Wegener G, Boetius A (2009) An experimental study on short-term changes in the anaerobic oxidation of methane in response to varying methane and sulfate fluxes. *Biogeosciences* 6(5):867–876.
46. Regnier P, et al. (2011) Quantitative analysis of anaerobic oxidation of methane (AOM) in marine sediments: A modeling perspective. *Earth Sci Rev* 106(1):105–130.
47. Wanninkhof R (1992) Relationship between wind speed and gas exchange over the ocean. *J Geophys Res Oceans* 97(C5):7373–7382.
48. Planavsky NJ, et al. (2010) The evolution of the marine phosphate reservoir. *Nature* 467(7319):1088–1090.
49. Ward B, Kilpatrick K, Novelli P, Scranton M (1987) Methane oxidation and methane fluxes in the ocean surface layer and deep anoxic waters. *Nature* 327(6119):226–229.
50. Etiope G, Sherwood Lollar B (2013) Abiotic methane on Earth. *Rev Geophys* 51(2): 276–299.